



Article scientifique

Article

2023

Published version

Open Access

This is the published version of the publication, made available in accordance with the publisher's policy.

New U-Pb baddeleyite ID-TIMS ages from the intrusive high-Ti-Sr rocks of the Southern Paraná LIP, Brazil: Implications for correlations with environmental disturbances during the Early Cretaceous

Rocha, Brenda C.; Gaynor, Sean; Janasi, Valdecir A.; Davies, Joshua H.F.L.; Florisbal, Luana M.; Waichel, Breno L.; Schaltegger, Urs

How to cite

ROCHA, Brenda C. et al. New U-Pb baddeleyite ID-TIMS ages from the intrusive high-Ti-Sr rocks of the Southern Paraná LIP, Brazil: Implications for correlations with environmental disturbances during the Early Cretaceous. In: Results in geochemistry, 2023, p. 100023. doi: 10.1016/j.ringeo.2023.100023

This publication URL: <https://archive-ouverte.unige.ch/unige:166499>

Publication DOI: [10.1016/j.ringeo.2023.100023](https://doi.org/10.1016/j.ringeo.2023.100023)

New U-Pb baddeleyite ID-TIMS ages from the intrusive high-Ti-Sr rocks of the Southern Paraná LIP, Brazil: Implications for correlations with environmental disturbances during the Early Cretaceous

Brenda C. Rocha¹, Sean P. Gaynor^{2,3}, Valdecir A. Janasi¹, Joshua H.F.L. Davies⁴, Luana M. Florisbal⁵, Breno L. Waichel⁵, Urs Schaltegger²

¹Departamento de Mineralogia e Geotectônica, Instituto de Geociências, Universidade de São Paulo, Brazil

²Département des sciences de la Terre, Université de Genève, Genève, Switzerland

³Department of Geosciences, Princeton University, Princeton, New Jersey, 08544, United States of America

⁴Département des Sciences de la Terre et de l'atmosphère/Geotop, Université du Québec à Montréal, Canada

⁵Programa de Pós-graduação em Geologia, Universidade Federal de Santa Catarina, Brazil

HIGHLIGHTS

- The *ca.* 132 Ma baddeleyite ages from high-Ti-Sr mafic intrusive rocks are equivalent within uncertainty and younger than previous estimates for the Florianópolis Dyke Swarm
- Younger ages can reflect Pb-loss
- Baddeleyite ID-TIMS datasets are complicated and require cautious interpretation, but can potentially be used to determine the timing of emplacement of mafic dykes and sills that are scarce in zircon.

Abstract

Large volumes of mafic igneous rocks are commonly emplaced during Large Igneous Province (LIP) eruptions, and these mafic rocks are often contemporaneous with periods of environmental disturbances, such as global ocean anoxia, and as a result, mass extinctions. The Paraná-Etendeka LIP is no exception, and has been previously correlated with, and interpreted to be the cause of the Valanginian oceanic anoxic event (OAE), a small global environmental disturbance. Here, we present new U-Pb ID-TIMS baddeleyite ages from high-Ti-Sr mafic intrusive rocks from the Paraná LIP, in Brazil. While these data are potentially complicated by the presence of Pb-loss and inheritance, it is possible to interpret geologically meaningful ages from them. The first high-precision age is reported for the type-locality of the Florianópolis Dyke Swarm, in North Santa Catarina Island, which yields an age of $132.53 \pm 0.40/0.40/0.42$ Ma. We also report an age of $132.07 \pm 0.27/0.30/0.33$ Ma for a dolerite sill, which intrudes organic-rich sedimentary rocks of the Paraná Basin. The emplacement of high-

Ti-Sr magmas at *ca.* 132 Ma suggests that there was up to 2 Myr of intrusive magmatism in the southern part of the Paraná LIP. Further investigation on the mafic intrusive magmatism from the Paraná LIP through robust high-precision geochronology is required to elucidate the proposed linkage more clearly with environmental changes during the Early Cretaceous.

1. Introduction

Large igneous provinces (LIPs) consist of large volumes of predominantly mafic lava flows and intrusive plumbing systems composed of dyke swarms, sill complexes and layered intrusions (Ernst, 2014). These magmatic events are typically characterized by a short duration (1-5 Myr) (e.g., Courtillot and Renne, 2003; Bryan and Ernst, 2008). LIP magmatism and its associated volatile gas release can cause global climatic disturbances that include global warming or cooling, and shifts in sea-water composition, all of which can lead to changes in global fauna, potentially at the mass extinction level (e.g., Ernst and Youbi, 2017; Black et al., 2021). The global impacts of LIPs can be caused by many aspects of their emplacement, such as volcanogenic gas release, thermogenic volatile production from contact metamorphism of volatile rich sediments, or drawdown of CO₂ and associated climatic cooling during weathering of fresh basaltic lava (e.g., Svensen et al., 2012; Cox et al., 2016; Heimdal et al., 2019), all of which can lead to significant modification of the atmosphere and ocean (e.g., Bond and Grasby, 2017). Volatile gas release can also cause perturbations to the global carbon cycle that result in ocean anoxia events (OAEs), which are preserved through black shale deposition (e.g., Jenkyns, 2010; Percival et al., 2015). The impact of individual LIPs on the environment varies due to many local factors, as well as the state of the climate at the time of LIP emplacement. For example, the release of greenhouse

gases and thermogenic volatiles (e.g., CO₂, CH₄, SO₂) from sediments during LIP emplacement may occur through the intrusion of LIP magmas into volatile-rich sediments such as organic-rich shales, coal and evaporites, either by assimilation (e.g., Heimdal et al., 2019, 2021; Davies et al., 2021) or contact metamorphism (e.g., Aarnes et al., 2010; Ganino and Arndt, 2010).

Synchronicity between the emplacement of the intrusive component of LIPs and periods of extreme climate perturbations leading to mass extinctions has been demonstrated for several LIPs, including the Siberian Traps (e.g., Burgess et al., 2017), CAMP (e.g., Blackburn et al., 2013, Davies et al., 2017), Karoo LIP (e.g., Svensen et al., 2012, Greber et al., 2020, Gaynor et al., 2022a) and Deccan Traps (e.g., Schoene et al. 2015; 2019, Sprain et al. 2019). However, recent work has also shown that some extreme carbon cycle variations that have been previously ascribed to LIP emplacement are temporally decoupled, and therefore unrelated (e.g., De Lena et al., 2019). High-precision geochronology is a key tool for temporally resolving the timescales of LIP magmatism and establishing causal relationships between individual LIPs and environmental change (e.g., Kasbohm et al., 2021).

The Cretaceous Paraná-Etendeka LIP, located in South America (mostly in Brazil) and Namibia, has an estimated total volume of at least 1,700,000 km³, which makes it one of the Earth's largest LIPs (Fig. 1; e.g., Frank et al., 2009). Despite the potential for significant volcanogenic output from this substantial magmatic province, the environmental effects associated with the Paraná-Etendeka LIP are minimal. The only global climatic event that has been temporally linked to this LIP is a minor oceanic anoxic event (OAE) during the Valanginian (e.g., Charbonnier et al., 2017; Svensen et al., 2018). The best estimate for the onset of the Valanginian Event is the youngest astronomical age of 135.22 ± 1.00 Ma from Martinez et al., (2015). Recently however,

this temporal link between the main volcanic phase of the Paraná LIP, the most voluminous South American portion of the Paraná-Etendeka LIP, and the Valanginian OAE event has been questioned, at least for the silicic parts of the province. The stratigraphically oldest low-Ti silicic magmas erupted rapidly at *ca.* 133.6 Ma based on high-precision, chemical abrasion ID- TIMS U-Pb zircon geochronology, and therefore postdate the Valanginian event by ~1 Myr (Rocha et al., 2020). However, the role of mafic intrusions in the Paraná LIP, some of which are stratigraphically older than the silicic magmatism, remains unclear due to limited high-precision geochronology from these rock types, and therefore our understanding the full time span of the LIP and the potential link with climate events is currently incomplete.

Here we present new high-precision baddeleyite U-Pb ID-TIMS data and whole-rock geochemistry data from high-Ti-Sr mafic intrusive rocks of the Paraná LIP. We analyzed baddeleyite from two samples representative of Paraná LIP intrusive magmatism (Figure 1): (i) the mafic component of a N20° composite dyke (VLF-07M – Figure 2a) from the North Santa Catarina Island, the type-locality of the Florianópolis Dyke Swarm (FDS), and (ii) a high-Ti-Sr dolerite sill (ITC-30 – Figures 1; 3a), up to 100m thick and named the Taió Sill (Waichel et al., 2019), emplaced in Permian-Triassic sedimentary rocks from the Paraná Basin, including organic-rich shales, pelites and sandstones. Additional field aspects, petrographic, geochemical, and isotopic information of sample VLF-07C, which represents a silicic rich core of the N20° composite dyke are provided in Florisbal et al. (2018). Using our new data, we improve our understanding of the timespan of the Paraná LIP and evaluate the potential connection between the intrusive phase of the Paraná LIP and Valanginian climate change.

2. Geological framework and previous geochronology data

The Cretaceous Paraná-Etendeka LIP is a continental flood basalt province, with *ca.* 917,000 km² (Frank et al., 2009) of exposed volcanic rocks, composed mainly of tholeiitic basalts (e.g., Bellieni et al., 1986; Peate, 1997). In the Paraná portion of the LIP, the earliest low-Ti basaltic flows in the southern domain are represented by the Gramado basalts, equivalent to the pahoehoe and rubbly pahoehoe flows of the Torres and Vale do Sol Formations, and the Esmeralda basalts (Figure 1; Peate, 1997; Rossetti et al., 2018). High-Ti-Sr Urubici magmas (Peate et al., 1999) are interbedded with low-Ti Gramado basalt flows in the lower portion of the lava pile (Peate, 1997; Peate et al., 1999). The low-Ti basalts are overlain by or interbedded with a sequence of low-Ti silicic volcanic rocks (Palmas-type), which are composed of chemically and stratigraphically distinct dacites and rhyolites (Bellieni et al., 1986; Peate, 1997; Nardy et al., 2008). This dominantly low-Ti volcanic sequence is covered by a younger sequence of high-Ti basalts (Pitanga and Paranapanema) and associated high-Ti silicic volcanics (Chapecó type) in the central and northern Paraná LIP (Ernesto et al., 1999; Nardy et al., 2008; Janasi et al., 2011). Pre-volcanic Paleozoic sediments from the Paraná basin (e.g., Canile et al., 2016) and Precambrian basement are intruded by abundant mafic sills and dykes forming the Florianópolis (Peate et al., 1990; Raposo et al., 1998; Florisbal et al., 2014, 2018), Ponta Grossa (Almeida et al., 2018) and Serra do Mar Dyke Swarms, which are interpreted as part of the plumbing system of the Paraná LIP (Figure 1).

The timing of the main magmatic activity in the Paraná LIP was previously estimated as 135-134 Ma, mostly based on ⁴⁰Ar-³⁹Ar ages from low-Ti basalts (Renne et al., 1992; Thiede and Vasconcelos, 2010; Gomes and Vasconcelos, 2021; Bacha et al., 2022), and these ages led several workers to attribute a causal-relationship between the

Paraná-Etendeka LIP and the 135.22 ± 1.00 Ma Valanginian Event (e.g., Erba et al., 2004; Thiede and Vasconcelos, 2010; Martinez et al., 2015; Charbonnier et al., 2017; Bacha et al., 2022). Less precise U-Pb secondary ion mass spectrometry (SIMS) ages from low-Ti andesite, high-Ti basalts and high-Ti silicic volcanics suggest crystallization at *ca.* 134 Ma (Pinto et al., 2011; Hartmann et al., 2019). Baddeleyite and zircon U-Pb ID-TIMS ages of *ca.* 134.7-133.4 Ma from the high-Ti Chapecó Ourinhos trachydacite (Janasi et al., 2011) and high-Ti-Sr Florianópolis (Florisbal et al., 2014) and Ponta Grossa dyke swarms (Almeida et al., 2018) are more precise, but were generated from multigrain fractions with high Pb blanks and could have unresolved Pb-loss. However, recent high-precision single grain U-Pb zircon geochronology using chemical abrasion to ensure the mitigation of Pb-loss (e.g., Mattinson, 2005; Widmann et al., 2019) indicates the low-Ti Palmas silicic magmas erupted rapidly at *ca.* 133.6 Ma within a short period of ~ 700 kyr, and therefore silicic magmatic activity postdates the Valanginian Event by ~ 1 Ma, at least in the southern and central part of the Paraná LIP (Rocha et al., 2020).

The age of basalt magmatism is still poorly constrained in the province and is based on less precise ^{40}Ar - ^{39}Ar data (see recent review by Gomes and Vasconcelos, 2021). The higher uncertainties from the existent dataset overlap within error with the youngest astronomical age of 135.22 ± 1.00 Ma available for the Valanginian Event (Martinez et al., 2015). The current U-Pb estimates for the mafic intrusions from the Florianópolis and Ponta Grossa Dyke Swarms based on zircon and baddeleyite TIMS data are within the *ca.* 134.7-133.4 Ma age range (Florisbal et al., 2014; Almeida et al., 2018) (Figure 1). A compilation of published ages of mafic rocks from the Paraná LIP is provided in the Supplementary Material (Table S1).

The coastal region of the Santa Catarina state, south Brazil, exposes abundant mafic (basalt to basaltic andesite) dykes, with rare occurrences of intermediate to felsic rocks (Marques et al., 1993; Raposo et al., 1998; Marques, 2001; Florisbal et al., 2014, 2018; Marques et al., 2018) which together are the Florianópolis Dyke Swarm (FDS). This is one of the major dyke swarms associated with the Paraná-Etendeka LIP and is dominated by high Ti-Sr-P basalts, interpreted as feeders of the unique Urubici (= Khumib) lavas of the Paraná and Etendeka lava piles (Peate et al., 1999; Ewart et al., 2004; Florisbal et al., 2014, 2018; Marques et al., 2018). The dykes have variable thicknesses (1 up to 10 m, some with more than 70 m), and are NNE (N15°-50°E) oriented, parallel to the coastline. All dykes intrude Neoproterozoic granites of the Florianópolis Batholith (Florisbal et al., 2014, 2018). The structural context and geochemistry of the dykes has been extensively studied (Marques et al., 1993; Raposo et al., 1998; Marques, 2001; Florisbal et al., 2014, 2018; Marques et al., 2018). The current estimates of the timing of their emplacement are mainly based on ^{40}Ar - ^{39}Ar ages from Raposo et al. (1998), who obtained two age periods of 131-127 Ma and 123-121 Ma for the Santa Catarina Island dykes (recalculated using the monitor ages of Kuiper et al., 2008). ID-TIMS U-Pb baddeleyite and zircon ages of ca. 134 Ma from two dykes of the high-Ti-Sr-P basaltic and trachyandesites dykes from Garopaba and Pinheira Beaches, south of the Santa Catarina Island led Florisbal et al. (2014) to question the ^{40}Ar - ^{39}Ar ages and the associated large age range for the FDS.

3. Methods

For whole-rock geochemistry, samples were crushed in a hydraulic press and powdered in an agate mill. Major and trace element concentration for sample VLF-07M

was obtained by x-ray fluorescence (XRF) spectrometry in fused disks after lithium metaborate/tetraborate fusion and pressed pellets, respectively at the NAP Geoanalítica laboratory, Universidade de São Paulo (USP) (Brazil), following the methods described in Mori et al. (1999). Additional trace element data, including the rare earth elements (REE) were obtained at the NAP Geoanalítica laboratory (USP) by inductively coupled plasma mass spectrometry (ICP-MS) using a Perkin Elmer Plasma Quadrupole MS Elan 6100DRC after dissolution of 40 mg of sample by acid digestion (HF+HNO₃) in Parr bombs for 5 days at 200 °C (see Navarro et al., 2008 for further details). Major and trace element composition, including the REE of sample ITC-30 were determined at Actlabs, Canada, by inductively coupled plasma optical emission spectrometry (ICP-OES) and ICP-MS, after metaborate/tetraborate fusion. Precision for major elements is better than 2%, and for trace elements is better than 10%. Whole-rock geochemistry data are reported in the Supplementary Material (Table S2).

Thin sections from samples VLF-07M and ITC-30 were investigated by backscattered electron imaging (BSE) to characterize the morphology, dimension, and textural setting of baddeleyite grains. Backscattered electron (BSE) images of baddeleyite were obtained using a FEI Quanta 600F Scanning Electron Microscope (SEM), with an accelerating voltage of 10-20 kV in high-vacuum mode, at the Technological Characterization Laboratory, Polytechnic School (LCT-USP).

For mineral separation, the samples were crushed in a tungsten mill, sieved to less than 300 µm, and then passed over a Wilfley table, using the water-based technique from Söderlund & Johansson, (2002). Magnetic minerals were removed from the fine mineral concentrate using a hand-magnet. Following Wilfley table separation, individual baddeleyite grains were handpicked under a binocular microscope using a pipette. Forty tiny dark brown baddeleyite blades were recovered from sample VLF-

07M. A few small-sized zircon grains ($<2 \mu\text{m}$) were extracted from sample ITC-30 but were unfortunately completely dissolved during the chemical abrasion procedure. Despite the lack of dateable zircon, sixteen tiny dark brown baddeleyite fragments were recovered from sample ITC-30. After picking, individual baddeleyite crystals underwent ultrasonic cleaning four times in 0.3 M HNO_3 in 3mL Savillex beakers to remove any superficial impurities without leaching the grains. Cleaned baddeleyite crystals were then loaded into individual 200 μl Savillex microcapsules along with approximately 70 μl of concentrated HF and trace HNO_3 . The grains were spiked with the EARTHTIME $^{202}\text{Pb} + ^{205}\text{Pb} + ^{233}\text{U} + ^{235}\text{U}$ tracer solution (calibration version 3; Condon et al., 2015; McLean et al., 2015) and placed into a Parr digestion vessel at 210 °C for 48 hours for dissolution. Following dissolution, the samples were dried and converted to a chloride form by placing them back in the oven overnight in 6 N HCl. The samples were dried again and re-dissolved in 3 N HCl and U and Pb were concentrated through anion exchange column chromatography using H_2O and HCl (Krogh, 1973). Once purified, the U and Pb fractions were combined in cleaned 7 ml Savillex beakers and dried down with weak H_3PO_4 , prior to loading on outgassed zone-refined Re ribbon filaments with a Si-gel emitter (modified from Gerstenberger & Haase, 1997).

Uranium and lead were measured on an IsotopX Phoenix TIMS mass spectrometer at the University of Geneva (Switzerland). Lead measurements were made in dynamic mode using a Daly photomultiplier, and U was measured as an oxide in static mode using Faraday cups coupled to $10^{12} \Omega$ resistors. The $^{18}\text{O}/^{16}\text{O}$ oxygen isotope composition of uranium oxide was determined to be 0.00205 based on replicate measurements of U500. Mass fractionation of Pb and U was corrected using the spike composition (Condon et al., 2015). The abundance of U was subsequently calculated

assuming a U isotopic composition of $^{238}\text{U}/^{235}\text{U} = 137.818 \pm 0.045$ (2σ) (Hiess et al., 2012). All common Pb was considered laboratory blank and was corrected using the long term blank isotopic composition at the University of Geneva (Schaltegger et al., 2021). All data were processed with the Tripoli and Redux U–Pb software packages (Bowring et al. 2011; McLean et al. 2011), and all ages were corrected for initial ^{230}Th disequilibrium in the melt using a U/Th ratio of the magma of 3.5. The EARTHTIME ET100Ma synthetic solution was also analyzed with the baddeleyite crystals and yielded a weighted mean $^{206}\text{Pb}/^{238}\text{U}$ age of 100.1762 ± 0.0056 Ma (MSWD = 2.0; n = 22), within uncertainty of the recently reported inter-laboratory calibrated value of 100.173 ± 0.003 Ma for this solution (Schaltegger et al., 2021; database at DOI:10/gk53tk). $^{206}\text{Pb}/^{238}\text{U}$ dates are reported with [X]/[Y]/[Z] uncertainties at the 2σ level, where X is the internal uncertainty, Y also includes the tracer calibration uncertainty plus internal uncertainty and Z includes the analytical uncertainty plus the tracer calibration and decay constant uncertainties (Schoene et al., 2006).

4. Results

The two samples analyzed, including the mafic component of a N20° composite dyke (VLF-07M; Florianópolis Dyke Swarm) and the high-Ti-Sr dolerite (ITC-30; Taió Sill) have tholeiitic basaltic compositions ($\text{SiO}_2 = 50.6\text{-}51.7$ wt%) and have similar MgO concentrations (MgO = 3.0-4.3 wt%) (Table S2). Both samples have high Ti ($\text{TiO}_2 = 3.08\text{-}3.55$ wt%) and Sr (519-553 ppm) contents. Sample VLF-07M is classified as a high-Ti Urubici magma-type (Figure 4), according to the criteria from Peate et al. (1992). The high-Ti-Sr dolerite sill (sample ITC-30) is characterized by high TiO_2 (> 3 wt %), Sr (> 550 ppm), Ba (> 600 ppm) and Zr (> 250 ppm), low MgO (3 wt %), but the high $\text{Fe}_2\text{O}_3(\text{t})$ (16.10 wt %) contents are not consistent with the Urubici magmas, as

highlighted by Peate et al. (1992). Despite the high Sr contents, sample ITC-30 mostly likely corresponds to the high-Ti Pitanga magma type (Peate et al., 1992) or alternatively the high-Ti transitional magma type (e.g., Marques et al., 2018).

Back-scattered electron (BSE) imaging reveals that baddeleyite from the mafic intrusive rocks often forms small (<10 μm), prismatic euhedral blades and are frequently found enclosed in matrix augite and in direct contact with quartz (Figs. 2b and 3b). All U-Pb ID-TIMS baddeleyite analyses (Table 1) yielded concordant Early Cretaceous Th-corrected $^{206}\text{Pb}/^{238}\text{U}$ ages (Figure 5), with the exception of one baddeleyite from sample VLF-07M which yielded a normally discordant Late Triassic $^{206}\text{Pb}/^{238}\text{U}$ date of 211.85 ± 0.42 Ma (Figure 5a). The remaining eight baddeleyite analyses from the high-Ti-Sr Urubici-type composite dyke from the Florianópolis Dyke Swarm (sample VLF-07M) yielded concordant $^{206}\text{Pb}/^{238}\text{U}$ dates ranging from 129.88 ± 0.88 to 138.41 ± 0.89 Ma (Figure 5b). A coherent plateau of dates at approximately 132 Ma, which excludes two slightly younger analyses and two anomalously older analyses, yielded a weighted mean $^{206}\text{Pb}/^{238}\text{U}$ age of $132.53 \pm 0.40/0.40/0.42$ Ma (MSWD = 0.27; $n = 2$) (Figure 6). The older date of 138.41 ± 0.89 Ma is an outlier that might represent a mixture between a potential xenocrystic zircon inclusion with autocrystic baddeleyite (see below).

Baddeleyite from the high-Ti-Sr dolerite mafic Taió Sill (sample ITC-30) yielded concordant $^{206}\text{Pb}/^{238}\text{U}$ dates ranging from 130.1 ± 1.31 to 132.40 ± 0.55 Ma (Figure 5c). Four of the five analyses overlap at approximately 132 Ma and yield a weighted mean $^{206}\text{Pb}/^{238}\text{U}$ age of $132.07 \pm 0.27/0.30/0.33$ Ma (MSWD = 0.65; $n = 4$) (Figure 6).

5. Discussion

5.1. Baddeleyite ages for Paraná intrusive magmatism

The U-Pb CA-ID-TIMS technique is usually regarded as the “gold standard” in geochronology, when using the EARTHTIME spikes, the data are calibrated to the SI unit, and the TIMS technique gives the analytical precision and accuracy to temporally resolve the timescales of LIP magmatism and evaluate potential causal relationships with global climatic and environmental disturbances (e.g., Davies et al., 2017, 2021; Schoene et al., 2019; Greber et al., 2020; Gaynor et al., 2022a). However, this “gold standard” of precision and accuracy is associated with chemically abraded zircon analyses, where the influence of Pb-loss has been removed or significantly reduced. Unfortunately, other minerals such as baddeleyite are not amenable to the chemical abrasion treatment applied to zircon (e.g., Rioux et al., 2010). Furthermore, geochronology of small baddeleyite crystals is particularly challenging due to the low abundances of U and radiogenic Pb in the analyses, resulting in low radiogenic to common lead ratios (Pb^*/Pb_c) of 1-4 for sample VCF-07M, and 1-2.7 for sample ITC-30. In Phanerozoic grains with low (Pb^*/Pb_c) values, $^{207}Pb/^{235}U$ ages are nearly one order of magnitude less precise than $^{206}Pb/^{238}U$ ages due to much lower concentrations of radiogenic ^{207}Pb relative to ^{206}Pb (e.g., Gaynor et al., 2022b). Perhaps counterintuitively, $^{207}Pb/^{235}U$ ages from Phanerozoic grains that have large measurement uncertainties due to low Pb^*/Pb_c are more likely to have error ellipses that overlap with the Concordia curve. For example, all baddeleyite crystals measured here except for grain b3 (which gives an age of ca. 211 Ma) (Figure 5b) are concordant. Therefore, any geological interpretation of age difference or age scatter needs to be applied with caution since concordance alone cannot necessarily be used as an interpretative guide of data quality or accuracy.

Both samples dated here yielded complicated, protracted U-Pb age spectra, which require interpretation to arrive at an estimate for the timing of emplacement. The close association of baddeleyite and quartz in the dated samples (Figs. 2, 3) supports the interpretation that baddeleyite autocrysts crystallized in and around evolved, SiO₂ saturated melt pockets, and therefore represents a metastable phase formed during late stage mafic magma evolution (e.g., Heaman and LeCheminant, 1993; Davies et al., 2021; Schaltegger and Davies, 2017). Natural examples and experiments indicate that metastable baddeleyite under silica-saturated conditions can occur on micron to submicron scales (Lewerentz et al., 2019). Also, the timeframe for emplacement and solidification within LIP intrusions is commonly short (*ca.* 500 yrs) (e.g., Davies et al., 2021) and is unlikely to be the origin of the age spread shown in the U-Pb data presented here.

The presence of anomalously old baddeleyite ²⁰⁶Pb/²³⁸U dates of 211.85 ± 0.42 Ma (grain b3) and 138.41 ± 0.89 (grain b5) from sample VLF-07M is difficult to explain as these ages are older than all previous ages of the Paraná-Etendeka LIP (e.g., Renne et al., 1992; Ernesto et al., 1999; Thiede and Vasconcelos, 2010; Janasi et al., 2011; Pinto et al., 2011; Florisbal et al., 2014; Almeida et al., 2018; Hartmann et al., 2019; Rocha et al., 2020, Gomes and Vasconcelos, 2021, Bacha et al., 2022). Baddeleyite antecrysts are essentially unknown and have not been previously described. Baddeleyite xenocrysts rarely form outside of highly alkaline melts such as kimberlites, alnoites and carbonatites (Heaman et al., 1992, Heaman and LeCheminant, 1993), since most primary melts are ZrO₂ undersaturated, therefore xenocrystic baddeleyite is not expected to be the cause of the old ages encountered here. Many mafic LIP intrusive rocks are known to contain xenocrystic zircon (Davies et al., 2021; Gaynor et al., 2022a) despite being zircon undersaturated (Boehnke et al., 2013; Bea et al., 2022). One

important mechanism for preserving zircon xenocrysts in mafic melts is contamination by melting of upper crustal lithologies during emplacement (e.g., Davies et al., 2021; Gaynor et al., 2022a). In the Paraná LIP, upper crustal lithologies are dominated by sandstones which contain detrital zircons with ages ranging from ~440 Ma to ~3 Ga (Canile et al., 2016), as well as Precambrian basement granitoids. These silica and zircon rich, potentially assimilated lithologies (see Peate et al., 1999; Florisbal et al., 2018) most likely melted rapidly during assimilation, resulting in Zr-rich local melt areas since Zr has a lower diffusivity than Si in mafic melts (Bea et al., 2022). Under certain conditions, the Zr-rich melt surrounding dissolving zircon could become saturated in ZrO₂ (baddeleyite), leading to the crystallization of baddeleyite. If this occurs before complete zircon dissolution, baddeleyite could nucleate on the dissolving zircon, encasing it and protecting it from further dissolution.

This mechanism has been proposed to explain baddeleyite with xenocrystic zircon cores from the Spread Eagle intrusive rocks (Pohlner et al., 2020) and is thought to occur in Ca-rich mafic melts (Lewerentz et al., 2019). This hypothesis was further supported by U-Pb SIMS dating of the zircon cores within baddeleyite from the Spread Eagle intrusions, which yielded older ²⁰⁶Pb/²³⁸U dates (Pohlner et al., 2020). Furthermore, detailed studies by Allibon et al. (2011) and Davies et al. (2017) also contain samples where baddeleyite crystals generate ages older than the proposed emplacement age of the rocks. Therefore, in spite of the lack of visual evidence for this process in our samples, we interpret that the older baddeleyite ages determined from the VLF-07M sample are the result of zircon xenocrystic inheritance. It does not take a large volume of inherited material to significantly disturb the U-Pb systematics (e.g., Gaynor et al., 2022b), and therefore the Th/U compositions of baddeleyite with zircon inclusions may not be significantly offset from those of pure baddeleyite due to

volumetric mixing, further obscuring the ability to detect inheritance. This process of xenocrystic inheritance in baddeleyite is poorly understood, due to factors like the limited analytical precision possible on small baddeleyite grains, where this process would be most easily observed, however it is likely more widespread than previously identified.

The final mechanism that is commonly invoked for dispersed baddeleyite age distributions is Pb-loss (e.g., Davies et al. 2015; Schaltegger and Davies, 2017 and Pohlner et al., 2020). Pb-loss can be effectively mitigated from zircon age spectra by applying chemical abrasion (Mattinson, 2005; Widmann et al., 2019). However, baddeleyite is not amenable to the chemical abrasion pre-treatment applied to zircon (Rioux et al., 2010), and therefore even pristine baddeleyite often displays small amounts of Pb-loss (e.g., Almeida et al., 2018; Pohlner et al., 2020; Davies et al., 2021; Gaynor et al., 2022a), which may be attributed to fast pathway diffusion in addition to volume diffusion (Pohlner et al., 2020). In cases where Pb-loss is suspected, a weighted mean $^{207}\text{Pb}/^{206}\text{Pb}$ age from all analyses may be calculated, to potentially rule out potential xenocrystic inheritance. In the case of VLF-07M, a weighted mean age for all of the analysis apart from the two older rejected analysis produces an imprecise $^{207}\text{Pb}/^{206}\text{Pb}$ age of 137.4 ± 30.4 Ma (2σ ; MSWD = 1.85), suggesting that these baddeleyite analyses do not reflect inheritance. However, for Phanerozoic samples, $^{207}\text{Pb}/^{206}\text{Pb}$ ages are too imprecise to allow a meaningful interpretation; the weighted mean upper intercept $^{207}\text{Pb}/^{206}\text{Pb}$ age for sample VLF-07M overlaps within uncertainty with all previous age constraints from the Paraná high Ti-Sr Urubici magmas. The $^{206}\text{Pb}/^{238}\text{U}$ dates from this sample have significantly higher scatter however, which we interpret to be the result of minor Pb-loss. We therefore suggest a more precise $^{206}\text{Pb}/^{238}\text{U}$ weighted mean age from oldest two baddeleyite analyses (excluding the

analyses with suspected zircon xenocryst influence and five analyses with suspected Pb-loss) of $132.53 \pm 0.40/0.40/0.42$ Ma (2σ ; MSWD = 0.27). It is possible that this age may still be affected by small degrees of Pb-loss, since it is one of the youngest U-Pb ages generated for the Paraná LIP. Sample ITC-30 yields a weighted mean $^{206}\text{Pb}/^{238}\text{U}$ age of $132.07 \pm 0.27/0.30/0.33$ Ma (MSWD = 0.65; $n = 4$) for the four oldest baddeleyite grains, which overlaps within uncertainty with the age from sample VLF-07M and is the best estimate for the emplacement of the Taió Sill (Figure 6).

5.2. Implications for the development of the Paraná LIP

The $132.53 \pm 0.40/0.40/0.42$ Ma age of sample VLF-07M is younger than previous U-Pb ID-TIMS ages of 134.7 ± 0.3 to 133.9 ± 0.7 Ma for the Florianópolis Dyke Swarm, which are interpreted as the feeders of the Urubici lavas (Florisbal et al., 2014). If dating the crystallization, the new ages reported here extend the age range for the high-Ti-Sr dykes to *ca.* 134–132 Ma and would indicate that intrusive magmatism in the southern part of the province occurred for up to 2 Myr. This time interval for the emplacement of the Paraná LIP is supported by previous geochronology (e.g., Renne et al., 1992, 1996a; Ernesto et al., 1999; Thiede and Vasconcelos, 2010; Janasi et al., 2011; Florisbal et al., 2014; Almeida et al., 2018; Rocha et al., 2020; this study) and by new paleomagnetic data from high-Ti sills and dykes (Ernesto et al., 2021).

Since baddeleyite dates may be biased by some degree of Pb-loss, it is possible that the younger baddeleyite ages of *ca.* 132.5 Ma reflect secondary Pb-loss, and therefore it is important to compare these data to previously published U-Pb geochronology. Previously published CA-ID-TIMS dates from a sample of the trachyandesite core of the Pinheira composite dyke range over 10 Myr however an upper intercept age of

133.89 ± 0.68 Ma was interpreted as the emplacement age, which is significantly older than the ages of this study (REF-02E; Florisbal et al., 2014). However, the previous U-Pb TIMS study was conducted using bulk grain fragments which were reported to have dark cores, a potential sign of xenocrystic inheritance. Due to the multi-grain nature of these analyses, volumetrically minor inheritance may have been overwhelmed by younger zircon crystallization, leading to subtly older but still concordant, data. Furthermore, this dataset includes an anomalously younger, normally discordant analyses, indicative of the presence of Pb-loss. Therefore, it is possible that these data are complicated by multiple factors that bias the dates away from the timing of crystallization, since applying an upper intercept approach to data with inheritance will yield an age older than the age of crystallization. Finally, we cannot directly compare these data to our new values, as these data were not reported with the uncertainties of their isotopic tracer solution. Instead, we suggest that the single grain analysis approach of our new data allows for a better evaluation of the age of these rocks and we suggest that further work is needed to better resolve the timing of the Paraná LIP.

The high precision baddeleyite ages of 132.53 ± 0.40/0.40/0.42 Ma and 132.07 ± 0.27/0.30/0.33 Ma reported here are also younger than Palmas low-Ti silicic volcanism (*ca.* 133.6 Ma) in Southern Paraná and Chapecó high-Ti silicic volcanism (*ca.* 132.9 Ma) at Central Paraná (Rocha et al., 2020), as well as a less precise ^{40}Ar - ^{39}Ar age of 133.3 ± 1.3 Ma from the earliest low-Ti basaltic flow in the Southern Paraná (Bacha et al., 2022). This indicates that at least some of the intrusive magmatism within the Paraná LIP postdates parts of its volcanism.

5.3. The relationship between the Valanginian global climate event and the Paraná

LIP

The Valanginian Event (Erba et al., 2004) has commonly been associated with the Paraná-Etendeka LIP volcanism due to some studies indicating temporal overlap (e.g., Thiede & Vasconcelos, 2010; Martinez et al., 2015; Charbonnier et al., 2017; Bacha et al., 2022), but this correlation is still controversial (Courtilot and Renne, 2003; Rocha et al., 2020). The apparent temporal correlation was due to the large uncertainties from the available ages of the Paraná-Etendeka, resulting in temporal overlap with the youngest astronomical age for the Valanginian Event (Martinez et al., 2015). Nevertheless, recent high-precision zircon single-grain ages have shown that the Paraná LIP low-Ti silicic volcanism, which is closely associated with the earliest low-Ti basalts, was not responsible for the minor environmental changes during the Valanginian, since it is younger than this OAE (Rocha et al., 2020). Regardless of the large magma volumes in the Paraná LIP ($\sim 600,000 \text{ km}^3$; Frank et al., 2009), the emplacement of mafic magmas into volatile-rich sediments that would potentially contribute to thermogenic gas release resulting in drastic environmental consequences, are very limited. Furthermore, very few robust geochronologic constraints from sills and dykes of the Paraná LIP are currently available to test this hypothesis (see Table S1). However, our new baddeleyite ages indicate that some intrusions within the Paraná LIP postdate the low-Ti silicic volcanism, suggesting that they were too young to have contributed to volcanogenic and thermogenic gases at the time of the Valanginian Event.

6. Summary and conclusions

The two baddeleyite ages of $132.53 \pm 0.40/0.40/0.42 \text{ Ma}$ and $132.07 \pm 0.27/0.30/0.33 \text{ Ma}$ obtained here from mafic intrusives are equivalent within uncertainty and are younger than previous age estimates from the Florianópolis Dyke Swarm. These

ages imply that the high-Ti-Sr magmas intrusive activity in the Southern Paraná LIP occurred over a period of up to 2 Myr. However, the possibility that these younger ages reflect secondary Pb-loss cannot be discarded. Baddeleyite high precision geochronology can be problematic in several aspects, in addition to the influence of Pb loss, analytical precision is also a critical limitation due to the typically small size of baddeleyite crystals in mafic rocks, with low abundances of U and radiogenic Pb. The present study highlights that baddeleyite ID-TIMS datasets are complicated and require cautious interpretation, but here we suggest that the ages data we have generated can potentially be used to determine the timing of emplacement of mafic dykes and sills that are scarce in zircon. Despite the fact that the Paraná-Etendeka LIP has been previously linked to a period of global climate disturbance, previous high precision U-Pb data as well as the new data presented here suggest that voluminous Paraná-Etendeka LIP volcanism may not have been the cause of the oceanic anoxic event during the Valanginian (Rocha et al., 2020). The mafic rocks of the Paraná LIP that intrude organic rich sediments could have had the potential to release thermogenic volatiles into the atmosphere, however, the results presented here reveal ages that are younger than the volcanic rocks, and the Valanginian anoxic event. Robust high-precision geochronology data is a prerequisite to evaluate the possible link between the mafic magma emplacement and environmental perturbations. Unfortunately, high precision U-Pb ages are very scarce in the Paraná LIP and additional data on mafic intrusive rocks are necessary.

Acknowledgments

This is part of the postdoc research of Brenda C. Rocha, with financial support from São Paulo Research Foundation (FAPESP) through grants 2016/23266-4 and

2019/24872-3, during her stay at the University of Geneva. This work was funded by São Paulo Research Foundation (FAPESP) grant 2019/22084-8 (to VAJ). Vasco Loios, Lucas Martins Lino and Thiago Vasconcelos are thanked for their assistance with sample preparation at CPGeo-USP. We thank David Peate and one anonymous reviewer for the thorough reviews that significantly helped to improve the clarity of the manuscript, Richard Ernst and Andrew Kerr for the editorial handling.

Declaration of interests

The authors declare that they have no known competing financial interests or personal relationships that could have appeared to influence the work reported in this paper.

References

- Aarnes, I., Svensen, H.H., Connolly, J.A.D., Podladchikov, Y.Y., 2010. How contact metamorphism can trigger global climate changes: modeling gas generation around igneous sills in sedimentary basins. *Geochimica et Cosmochimica Acta* 74, 7179-7195.
- Allibon, J., Ovtcharova, M., Bussy, F., Cosca, M., Schaltegger, U., Bussien, D., Lewin, E., 2011. Lifetime of an ocean island volcano feeder zone: constraints from U-Pb dating on coexisting zircon and baddeleyite, and ^{40}Ar - ^{39}Ar age determinations, Fuerteventura, Canary Islands. *Canadian Journal of Earth Sciences* 48 (2), 567-592.
- Almeida, V.V., Janasi, V.A., Heaman, L.M., Shaulis, B.J., Hollanda, M.H.B.M., Renne, P., 2018. Contemporaneous alkaline and tholeiitic magmatism in the Ponta Grossa Arch, Paraná-Etendeka Magmatic Province: constraints from precise U-Pb

- zircon/baddeleyite and ^{40}Ar - ^{39}Ar phlogopite dating of the José Fernandes Gabbro and mafic dykes. *Journal of Volcanology and Geothermal Research* 355, 55-65, doi:10.1016/j.jvolgeores.2017.01.018.
- Bacha, R.R.B., Waichel, B.L., Ernst, R.E., 2022. The mafic volcanic climax of the Paraná-Etendeka large igneous province as the trigger of the Weissert Event. *Terra Nova* 34(1), 28-36.
- Bea, F., Bortnikov, N., Cambeses, A., Chakraborty, S., Molina, J.F., Montero, P., Morales, I., Silantiev, S., Zinger, T., 2022. Zircon crystallization in low-Zr mafic magmas: Possible or impossible? *Chemical Geology* 602, 120898.
- Bellieni, G., Comin-Chiaramonti, P., Marques, L.S., Melfi, A.J., Nardy, A.J.R., Papatrechas, C., Piccirillo, E.M., Roisenberg, A., Stolfa, D., 1986. Petrogenetic aspects of acid and basaltic lavas from the Paraná Plateau (Brazil): geological, mineralogical and petrochemical relationships. *J. Petrol.* 27, 915–944.
- Black, B.A., Karlstrom, L., Mather, T.A., 2021. The life cycle of large igneous provinces. *Nature Reviews Earth & Environment*, 1-18.
- Blackburn, T.J., Olsen, P.E., Bowring, S.A., McLean, N.M., Kent, D.V., Puffer, J., McHone, G., Rasbury, E.T., Et-Touhami, M., 2013. Zircon U-Pb geochronology links the End-Triassic extinction with the Central Atlantic Magmatic Province. *Science* 340, 941-945.
- Boehnke, P., Watson, E.B., Trail, D., Harrison, T.M., Schmitt, A.K., 2013. Zircon saturation re-revisited. *Chemical Geology* 351, 324-334.
- Bond, D.P.G., Grasby, S.E., 2017. On the causes of mass extinctions. *Palaeogeography, Palaeoclimatology, Palaeoecology* 478, 3-29.

- Bowring, J.F., McLean, N.M., Bowring, S.A., 2011, Engineering cyber infrastructure for U-Pb geochronology: Tripoli and U-Pb Redux: *Geochemistry, Geophysics, Geosystems* 12 (6), 1-19.
- Bryan, S.E., and Ernst, R.E., 2008. Revised definition of Large Igneous Provinces (LIPs). *Earth-Science Reviews* 86 (1-4), 175-202.
- Burgess, S.D., Muirhead, J.D., Bowring, S.A., 2017, Initial pulse of Siberian Traps sills as the trigger of the end-Permian mass extinction. *Nature Communications* 8, 164, doi:10.1038/s41467-017-00083-9.
- Burgess, S.D., Bowring, S.A., Fleming, T.H., Elliot, D.H., 2015. High-precision geochronology links the Ferrar large igneous province with early-Jurassic Ocean anoxia and biotic crisis. *Earth and Planetary Science Letters* 415, 90-99.
- Canile, F.M., Babinski, M., Rocha-Campos, A.C., 2016. Evolution of the Carboniferous-Early Cretaceous units of Paraná Basin from provenance studies based on U-Pb, Hf and O isotopes from detrital zircons. *Gondwana Research* 40, 142-169.
- Charbonnier, G., Morales, C., Duchamp-Alphonse, S., Westermann, S., Adate, T., Föllmi, K.B., 2017. Mercury enrichment indicates volcanic triggering of Valanginian environmental change: *Scientific Reports* 7, 40808, doi:10.1038/srep40808.
- Condon, D., Schoene, B., McLean, N.M., Bowring, S.A., Parrish, R.R., 2015, Metrology and traceability of U-Pb isotope dilution geochronology (EARTHTIME Tracer Calibration Part I). *Geochimica et Cosmochimica Acta* 164, 464-480.
- Courtillot, V.E., and Renne, P.R., 2003. On the ages of flood basalt events. *Comptes Rendus Geoscience* 335 (1), 113-140.

- Cox, G.M., Halverson, G.P., Stevenson, R.K., Vokaty, M., Poirier, A., Kunzmann, M., Li, Z-X., Denyszyn, S.W., Strauss, J.V., Macdonald, F.A., 2016. Continental flood basalt weathering as a trigger for Neoproterozoic Snowball Earth. *Earth and Planetary Science Letters* 446, 89-99.
- Davies, J.H.F.L., Marzoli, A., Bertrand, H., Youbi, N., Ernesto, M., Greber, N.D., Ackerson, M., Simpson, G., Bouvier, A., -S., Baumgartner, L., Pettke, T., Farina, F., Ahrenstedt, H.V., Schaltegger, U., 2021. Zircon petrochronology in large igneous provinces reveals upper crustal contamination processes: new U-Pb ages, Hf and O isotopes, and trace elements from the Central Atlantic Magmatic Province (CAMP). *Contributions to Mineralogy and Petrology* 176(1), 1-24.
- Davies, J.H.F.L., Marzoli, A., Bertrand, H., Youbi, N., Ernesto, M., Schaltegger, U., 2017. End-Triassic mass extinction started by intrusive CAMP activity. *Nature Communications* 8, 15596, doi:0.1038/ncomms15596.
- Davies, J.H.F.L., Stern, R., Heaman, L.M., Rojas, X., Walton, E.L., 2015. Resolving oxygen isotopic disturbance in zircon: a case study from the low $\delta^{18}\text{O}$ Scourie dikes, NW Scotland. *American Mineralogist* 100, 1952-1966.
- De Lena, L.F., Taylor, D., Guex, J., Bartolini, A., Adatte, T., van Acken D., Spangenberg, J.E., Samankassou, E., Vennemann, T., Schaltegger, U., 2019, The driving mechanisms of the carbon cycle perturbations in the late Pliensbachian (Early Jurassic). *Scientific Reports* 9, 1-12.
- Erba, E., Bartolini, A., Larson, R.L., 2004. Valanginian Weissert oceanic anoxic event. *Geology* 32, 149–152, doi:10.1130/G20008.1.
- Ernesto, M., Zaffani, L.A., Caminha-Maciél, G., 2021. New paleomagnetic data from the Paraná Magmatic Province: brief emplacement time and tectonism. *Journal of South American Earth Sciences* 106, 102869.

- Ernesto, M., Raposo, M.I.B., Marques, L.S., Renne, P.R., Diogo, L.A., de Min, A., 1999. Paleomagnetism, geochemistry and $^{40}\text{Ar}/^{39}\text{Ar}$ dating of the North-eastern Paraná Magmatic Province: tectonic implications. *Journal of Geodynamics* 28 (4–5), 321–340.
- Ernst, R.E., 2014. *Large Igneous Provinces*. Cambridge University Press, Cambridge.
- Ernst, R.E., Youbi, N., 2017. How Large Igneous Provinces affect global climate, sometimes cause mass extinctions, and represent natural markers in the geological record. *Palaeogeography, Palaeoclimatology, Palaeoecology* 478, 30-52, doi: 10.1016/j.palaeo.2017.03.014.
- Ewart, A., Marsh, J.S., Milner, S.C., Duncan, A.R., Kamber, B.S., Armstrong, R.A., 2004. Petrology and geochemistry of early Cretaceous bimodal continental flood volcanism of the NW Etendeka, Namibia. Part 1: Introduction, mafic lavas and re-evaluation of mantle source components. *Journal of Petrology* 45(1), 59-105.
- Florisbal, L.M., Heaman, L.M., Janasi, V.A., Bitencourt, M.F., 2014. Tectonic significance of the Florianópolis Dyke Swarm, Paraná-Etendeka Magmatic Province: a reappraisal based on precise U-Pb dating. *Journal of Volcanology and Geothermal Research* 289, 140-150.
- Florisbal, L.M., Janasi, V.A., Bitencourt, M.F., Nardi, L.V.S., Marteleto, N.S., 2018. Geological, geochemical and isotope diversity of ~134 Ma dykes from the Florianópolis Dyke Swarm, Paraná Magmatic Province: Geodynamic controls on petrogenesis. *Journal of Volcanology and Geothermal Research* 355, 181-203.
- Frank, H.T., Elisa, M., Gomes, B., Luiz, M., Formoso, L., 2009. Review of the areal extent and the volume of the Serra Geral Formation, Paraná Basin, South America. *Pesquisas em Geociências* 36 (1), 49-57.
- Ganino, C., Arndt, N.T., 2009. Climate changes caused by degassing of sediments

- during the emplacement of large igneous provinces. *Geology* 37(4), 323-326, doi:10.1130/G25325A.1.
- Gaynor, S.P., Svensen, H.H., Polteau, S., Schaltegger, U., 2022a. Local melt contamination and global climate impact: dating the emplacement of Karoo LIP sills into organic-rich shale. *Earth and Planetary Science Letters* 579, 117371.
- Gaynor, S.P., Ruiz, M., Schaltegger, U., 2022b. The importance of high-precision in the evaluation of U-Pb zircon age spectra. *Chemical Geology* 603, 120913.
- Gerstenberger, H., Haase, G., 1997. A highly effective emitter substance for mass spectrometric Pb isotope ratio determinations. *Chemical Geology* 136, 309-312.
- Gomes, A.S., Vasconcelos, P.M., 2021. Geochronology of the Paraná-Etendeka large igneous province. *Earth-Science Reviews* 220, 103716.
- Greber, N.D., Davies, J.H.F.L., Gaynor, S.P., Jourdan, F., Bertrand, H., Schaltegger, U., 2020. New high precision U-Pb ages and Hf isotope data from the Karoo large igneous province; implications for pulsed magmatism and early Toarcian environmental perturbations. *Results in Geochemistry* 1, 100005.
- Hartmann, L.A., Baggio, S.B., Brückmann, M.P., Knijnik, D.B., Lana, C., Massone, H.J., Opitz, J., Pinto, V.M., Sato, K., Tassinari, C.C.G., Arena, K., 2019. U-Pb geochronology of Paraná volcanics combined with trace element geochemistry of the zircon crystals and zircon Hf isotope data. *Journal of South American Earth Sciences* 89, 219-226.
- Heaman, L.M., LeCheminant, A.N., 1993. Paragenesis and U-Pb systematics of baddeleyite (ZrO₂). *Chemical Geology* 110, 95-126.
- Heaman, L.M., LeCheminant, A.N., Rainbird, R.H., 1992. Nature and timing of Franklin igneous events, Canada: implications for a Late Proterozoic mantle plume and the break-up of Laurentia. *Earth and Planetary Science Letters* 109,

117-131.

- Heimdal, T.H., Callegaro, S., Svensen, H.H., Jones, M.T., Pereira, E., Planke, S., 2019. Evidence for magma-evaporite interactions during the emplacement of the Central Atlantic Magmatic Province (CAMP) in Brazil. *Earth and Planetary Science Letters* 506, 476-492.
- Heimdal, T.H., Jones, M.T., Svensen, H.H., 2020. Thermogenic gas release from the Central Atlantic magmatic province caused major end-Triassic carbon cycle perturbations. *Proceedings of the National Academy of Sciences* 177 (22), 11968-11974.
- Heimdal, T.H., Godd ris, Y., Jones, M.T., Svensen, H.H., 2021. Assessing the importance of thermogenic degassing from the Karoo Large Igneous Province (LIP) in driving Toarcian carbon cycle perturbations. *Nature Communications* 12, 6221.
- Hiess, J., Condon, D.J., McLean, N., Noble, S.R., 2012, $^{238}\text{U}/^{235}\text{U}$ systematics in terrestrial uranium-bearing minerals. *Science* 335, 1610-1614.
- Jaffey, A.H., Flynn, K.F., Glendenin, L.E., Bentley, W.C., and Essling, A.M., 1971, Precision measurement of half-lives and specific activities of ^{235}U and ^{238}U . *Physical Review C* 4, 1889-1906.
- Janasi, V.A., Freitas, V.A., Heaman, L.H., 2011. The onset of flood basalt volcanism, Northern Paran  Basin, Brazil: a precise U–Pb baddeleyite/zircon age for a Chapec -type dacite. *Earth and Planetary Science Letters* 302(1–2), 147–153, doi: 10.1016/j.epsl.2010.12.005.
- Jenkyns, H.C., 2010. Geochemistry of oceanic anoxic events. *Geochemistry, Geophysics, Geosystems* 11 (3), Q03004.
- Kasbohm, J., Schoene, B., Burgess, S., 2021. Radiometric constraints on the timing,

- tempo, and effects of Large Igneous Province emplacement. In: Ernst, R., Dickson, A.J., Bekker, A. (Eds.), Large Igneous Provinces: a driver of global environmental and biotic changes, American Geophysical Union and John Wiley and Sons, p. 27-82.
- Krogh, T. E., 1973, A low-contamination method for hydrothermal decomposition of zircon and extraction of U and Pb for isotopic age determinations. *Geochim. Cosmochim. Acta* 37, 485–494.
- Kuiper, K.F., Deino, A., Hilgen, F.J., Krijgsman, W., Renne, P.R., Wijbrans, J.R., 2008. Synchronizing rock clocks of Earth history. *Science* 320, 500-504, doi: 10.1126/science.1154339.
- Lewerentz, A., Harlov, D., Scherstén, A., Whitehouse, M.J., 2019. Baddeleyite formation in zircon by Ca-bearing fluids in silica-saturated systems in nature and experiment: resetting of the U-Pb geochronometer. *Contributions to Mineralogy and Petrology* 174: 64.
- Lucchetti, A.C.F., Nardy, A.J.R., Madeira, J., 2018. Silicic, high- to extremely high-grade ignimbrites and associated deposits from the Paraná Magmatic Province, southern Brazil: *Journal of Volcanology and Geothermal Research* 355, 270-286.
- Marques, L.S., 2001. Geoquímica dos diques toleíticos da costa sul-sudeste do Brasil: contribuição ao conhecimento da Província Magmática do Paraná. Livre-Docência Thesis. Universidade de São Paulo, São Paulo.
- Marques, L.S., Bellieni, G., De Min, A., Piccirillo, E.M., 1993. O enxame de diques da Ilha de Santa Catarina: resultados geoquímicos preliminares. IV Congresso Brasileiro de Geoquímica, Resumos, pp. 3–4.
- Marques, L.S., De Min, A., Rocha-Júnior, E.R.V., Babinski, M., Bellieni, G., Figueiredo, A.M.G., 2018. Elemental and Sr-Nd-Pb isotope geochemistry of the

- Florianópolis Dyke Swarm (Paraná Magmatic Province): crustal contamination and mantle source constraints. *Journal of Volcanology and Geothermal Research* 355, 149-164.
- Martinez, M., Deconinck, J.F., Pellenard, P., Riquier, L., Company, M., Reboulet, S., Moiroud, M., 2015. Astrochronology of the Valanginian-Hauterivian stages (Early Cretaceous): Chronological relationships between the Paraná-Etendeka large igneous province and the Weissert and the Faraonic events. *Global and Planetary Change* 131, 158-173, doi: 10.1016/j.gloplacha.2015.06.001.
- Mattinson, J., 2005, Zircon U-Pb chemical abrasion (“CA-TIMS”) method: combined annealing and multi-step partial dissolution analysis for improved precision and accuracy of zircon ages. *Chemical Geology* 220, 47-66.
- McLean, N.M., Bowring, J.F., Bowring, S.A., 2011, An algorithm for U-Pb isotope dilution data reduction and uncertainty propagation. *Geochemistry, Geophysics, Geosystems* 12 (6), 1-26.
- McLean, N.M., Condon, D.J., Schoene, B., Bowring, S.A., 2015, Evaluating uncertainties in the calibration of isotopic reference materials and multi-element isotopic tracers (EARTHTIME Tracer Calibration Part II). *Geochimica and Cosmochimica Acta* 164, 481–501.
- Mori, P.E., Reeves, S., Correia, C.T., Haukka, M., 1999. Development of a fused glass disc XRF facility and comparison with the pressed powder technique at Instituto de Geociências, Universidade de São Paulo. *Revista Brasileira de Geociências* 29, 441-446.
- Nardy, A.J.R., Machado, F.B., Oliveira, M.A.F., 2008, As rochas vulcânicas mesozóicas ácidas da Bacia do Paraná: litoestratigrafia e considerações geoquímico-estratigráficas. *Revista Brasileira de Geociências* 38, 178–195.

- Peate, D.W., 1997. The Paraná–Etendeka Province, *in*: Mahoney, J.J., Coffin, M.F., eds., Large Igneous Provinces: Continental, Oceanic, and Planetary Flood Volcanism, v.100, American Geophysical Union, 217–245.
- Peate, D.W., Hawkesworth, C.J., Mantovani, M.S.M., Shukowsky, W., 1990. Mantle-plumes and flood-basalt stratigraphy in the Paraná, South America. *Geology* 18, 1223-1226, doi: [10.1130/0091-7613\(1990\)018<1223:MPAFBS>2.3.CO;2](https://doi.org/10.1130/0091-7613(1990)018<1223:MPAFBS>2.3.CO;2).
- Peate, D.W., Hawkesworth, C.J., Mantovani, M.M.S., Rogers, N.W., Turner, S.P., 1999. Petrogenesis and stratigraphy of the high-Ti/Y Urubici magma type in the Paraná flood basalt province and implications for the nature of “Dupal”-type mantle in the South Atlantic Region. *Journal of Petrology* 40(3), 451-473.
- Percival, L.M.E., Witt, M.L.I., Mather, T.A., Hermoso, M., Jenkyns, H.C., Hesselbo, S.P., Al-Suwaidi, A.H., Storm, M.S., Ruhl, M., 2015. Globally enhanced mercury deposition during the end-Pliensbachian extinction and Toarcian OAE: a link to the Karoo-Ferrar Large Igneous Province. *Earth and Planetary Science Letters* 428, 267–280, doi: [10.1016/j.epsl.2015.06.064](https://doi.org/10.1016/j.epsl.2015.06.064).
- Pinto, V.M., Hartmann, L.A., Santos, J.O.S., McNaughton, N.J., Wildner, W., 2011, Zircon U–Pb geochronology from the Paraná bimodal volcanic province support a brief eruptive cycle at ~135 Ma. *Chemical Geology* 281(1–2), 93–102, doi: [10.1016/j.chemgeo.2010.11.031](https://doi.org/10.1016/j.chemgeo.2010.11.031).
- Pohlner, J.E., Schmitt, A.K., Chamberlain, K.R., Davies, J.H.F.L., Hildenbrand, A., Austermann, G., 2020. Multimethod U-Pb baddeleyite dating: insights from the Spread Eagle Intrusive Complex and Cape St. Mary’s sills, Newfoundland, Canada. *Geochronology* 2, 187-208.
- Raposo, M.I.B., Ernesto, M., Renne, P.R., 1998. Paleomagnetism and dating of the early Cretaceous Florianópolis dike swarm (Santa Catarina Island), Southern

- Brazil. *Physics of the Earth and Planetary Interior* 108 (4), 275–290.
- Renne, P.R., Ernesto, M., Pacca, I.G., Coe, R.S., Glen, J.M., Prévot, M., Perrin, M., 1992. The age of Parana flood volcanism, rifting of Gondwanaland, and the Jurassic–Cretaceous boundary. *Science* 258, 975–979.
- Renne, P.R., Deckart, K., Ernesto, M., Féraud, G., Piccirillo, E.M., 1996. Age of the Ponta Grossa dike swarm (Brazil), and implications to Paraná flood volcanism. *Earth and Planetary Science Letters* 144, 199–211.
- Rioux, M., Bowring, S., Dudás, F., Hanson, R., 2010. Characterizing the U–Pb systematics of baddeleyite through chemical abrasion: application of multi-step digestion methods to baddeleyite geochronology. *Contributions to Mineralogy and Petrology* 160, 777–801. doi.org/10.1007/s00410-010-0507-1
- Rocha, B.C., Davies, J.H.F.L., Janasi, V.A., Schaltegger, U., Nardy, A.J.R., Greber, N.D., Lucchetti, A.C.F., Polo, L.A., 2020. Rapid eruption of silicic magmas from the Paraná Magmatic Province (Brazil) did not trigger the Valanginian event. *Geology* 48, 1174-1178, doi.org/10.1130/G47766.1.
- Rossetti, L., Lima, E.F., Waichel, B.L., Hole, M.J., Simões, M.S., Scherer, C.M.S., 2018, Lithostratigraphy and volcanology of the Serra Geral Group, Paraná-Etendeka Igneous Province in southern Brazil: towards a formal stratigraphical framework: *Journal of Volcanology and Geothermal Research* 355, 98-114.
- Schaltegger, U., Davies, J.H.F.L., 2017. Petrochronology of zircon and baddeleyite in igneous rocks: reconstructing magmatic processes at high temporal resolution, *in*: Kohn, M. J., Engi, M., Lanari, P., eds., *Petrochronology*. Mineralogical Society of America. *Reviews in Mineralogy and Geochemistry* 83(1), 297-328, doi.org/10.2138/rmg.2017.83.10.

- Schaltegger, U., Ovtcharova, M., Gaynor, S.P., Schoene, B., Wotzlaw, J., Davies, J.H.F.L., Farina, F., Greber, N., Szymanowski, D., Chelle-Michout, C., 2021. Long-term repeatability and interlaboratory reproducibility of high-precision ID-TIMS U-Pb geochronology. *Journal of Analytical Atomic Spectrometry* 36, 1466-1477.
- Schoene, B., Crowley, J.L., Condon, D.J., Schmitz, M.A., Bowring, S.A., 2006. Reassessing the uranium decay constants for geochronology using ID-TIMS U-Pb data: *Geochimica et Cosmochimica Acta* 70, 426-445, doi: 10.1016/j.gca.2005.09.007.
- Schoene, B., Samperton, K.M., Eddy, M.P., Keller, G., Adatte, T., Bowring, S.A., Khadri, S.F., Gertsch, B., 2015. U-Pb geochronology of the Deccan Traps and relation to the end-Cretaceous mass extinction. *Science* 347, 182-184.
- Schoene, B., Eddy, M.P., Samperton, K.M., Keller, C.B., Keller, G., Adatte, T., Khadri, S.F.R. 2019. U-Pb constraints on pulsed eruption of the Deccan Traps across the end-Cretaceous mass extinction. *Science* 363 (6429), 815-816.
- Söderlund, U., Johansson, L., 2002. A simple way to extract baddeleyite (ZrO₂): *Geochemistry, Geophysics, Geosystems* 3 (2), 1-7.
- Sprain, C.J., Renne, P.R., Vanderkluysen, L., Pande, K., Self, S., Mittal, T., 2019. The eruptive tempo of Deccan volcanism in relation to the Cretaceous-Paleogene boundary. *Science* 363, 866-870.
- Svensen, H.H., Corfu, F., Polteau, S., Hammer, O., Planke, S., 2012. Rapid magma emplacement in the Karoo Large Igneous Province. *Earth and Planetary Science Letters* 325-326, 1-9.
- Svensen, H.H., Torsvik, T.H., Callegaro, S., Augland, L., Heimdal, T.H., Jerram, D.A., Planke, S., Pereira, E., 2018. Gondwana Large Igneous Provinces: plate

reconstructions, volcanic basins and sills volumes, *in* Sensarma, S., Storey, B.C., eds., Large Igneous Provinces from Gondwana and Adjacent Regions, Geological Society, London, Special Publications 463, doi: 10.1144/SP463.7.

Thiede, D.S., Vasconcelos, P.M., 2010. Parana flood basalts: rapid extrusion hypothesis confirmed by new $^{40}\text{Ar}/^{39}\text{Ar}$ results. *Geology* 38(8), 747–750, doi: 10.1130/G30919.1.

Waichel, B.L., Mouro, L.D., Vieira, L. D., Silva, M. S., Muller, C. 2019. The Taió plumbing system (Paraná-Etendeka igneous province, Southern Brazil)-Mapping, petrography and geochemistry. In: LASI , Malargue. LASI6 Scientific Programme. Malargue, 2019. v. 1.

Widmann, P., Davies, J.H.F.L., Schaltegger, U., 2019. Calibrating chemical abrasion: its effects on zircon crystal structure, chemical composition and U-Pb age. *Chemical Geology* 511, 1-10, doi: 10.1016/j.chemgeo.2019.02.026.

FIGURE CAPTIONS

Figure 1: Geological map of the Paraná LIP, showing the location of dated samples by U-Pb ID-TIMS (modified from Janasi et al., 2011; Lucchetti et al.; 2018, Rocha et al., 2020) and previous geochronology data from mafic intrusive rocks (Ernesto et al., 1999; Thiede and Vasconcelos, 2010; Florisbal et al., 2014; Almeida et al., 2018) (see Table S1 for database).

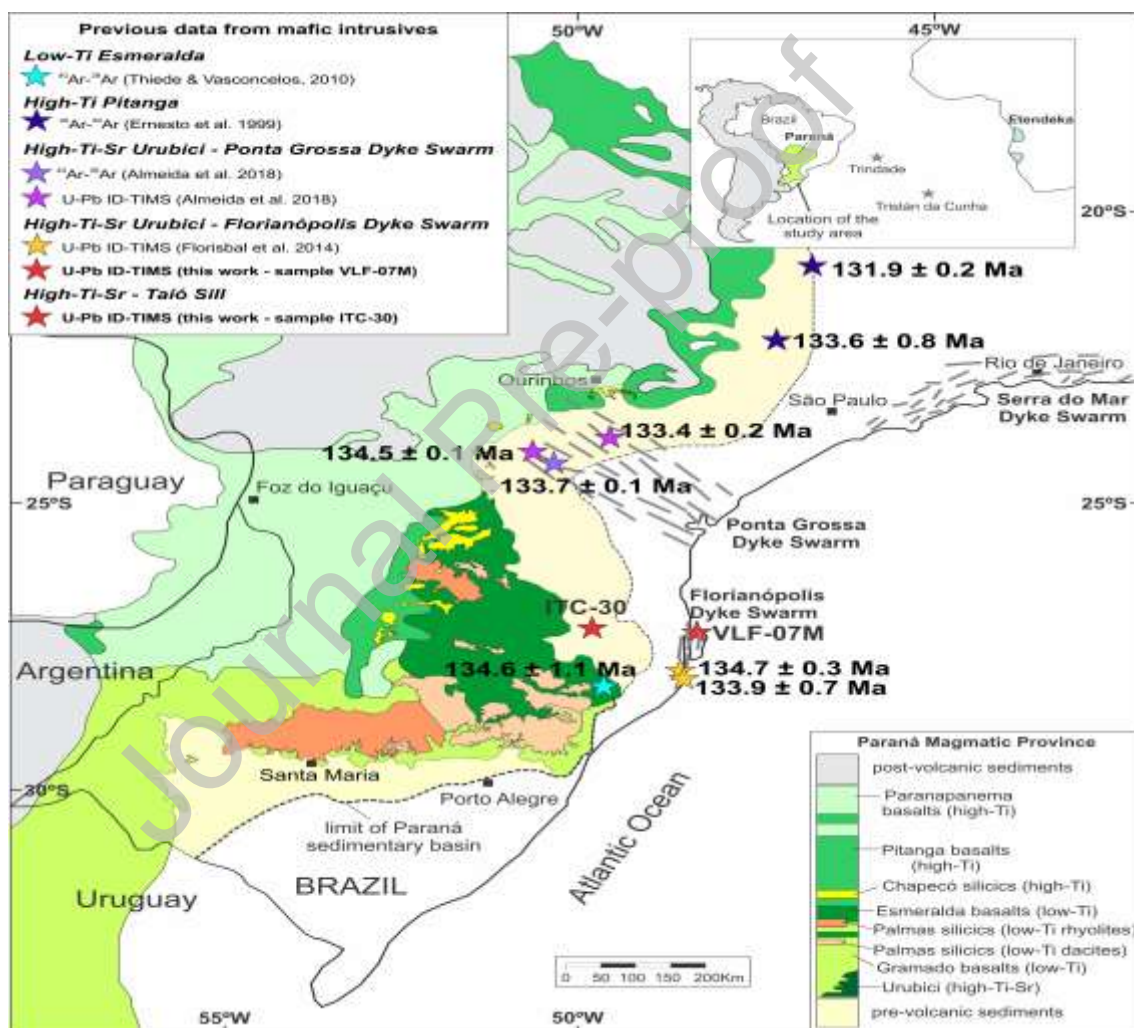


Figure 2: a) Field exposure of the Urubici-type high-Ti-Sr N20⁰ composite dyke (sample VLF-07M; coordinates: 48°24'19.635"W and 27°24'18.774"S), located at the North Santa Catarina Island, Brava Beach. The composite dyke has silicic core with xenoliths of granitic and metamorphic rocks and a basaltic rim 1-1.5 m thick with discrete cm sized chilled margins and sharp contacts with the leucogranitic facies of the Ilha Granite host rock (*ca.* 590 Ma). b) Back-scattered electron (BSE) image of fine-grained baddeleyite (<10 μm) enclosed in matrix augite from a mafic part of a high-Ti-Sr Urubici-type composite dyke (sample VLF-07M).



Figure 3: a) Field photo of the high-Ti-Sr dolerite mafic sill, which is up to 30 m thick (sample ITC-30; coordinates: 50°03'30.155"W and 27°04'20.183"S) and cutting sedimentary rocks from the Paraná Basin (shales, pelites and sandstones from the Irati, Teresina and Serra Alta Formations). b) Back-scattered electron (BSE) image of prismatic euhedral baddeleyite (<5 μm) enclosed in matrix augite and quartz, from the dolerite mafic Taió Sill (sample ITC-30).

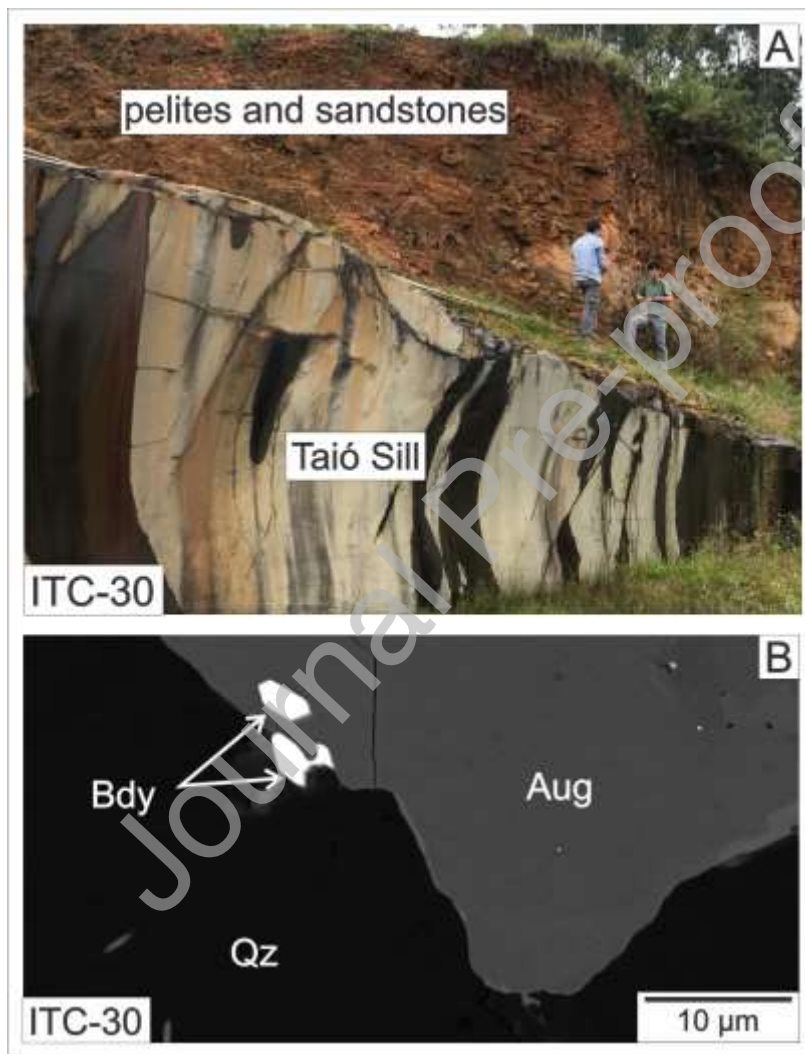


Figure 4: Selected variation diagrams for classification and distinction between magma types (Peate et al., 1992). a) MgO vs TiO₂ and b) Sr vs Zr/Y. Sample VLF-07M (Florianópolis Dyke Swarm) and ITC-30 (Taió Sill) are plotted as filled orange circle and filled blue circle, respectively. Data for Urubici-type rocks (filled red circles) are from Peate et al. (1999) and Florisbal et al. (2018), for comparison.

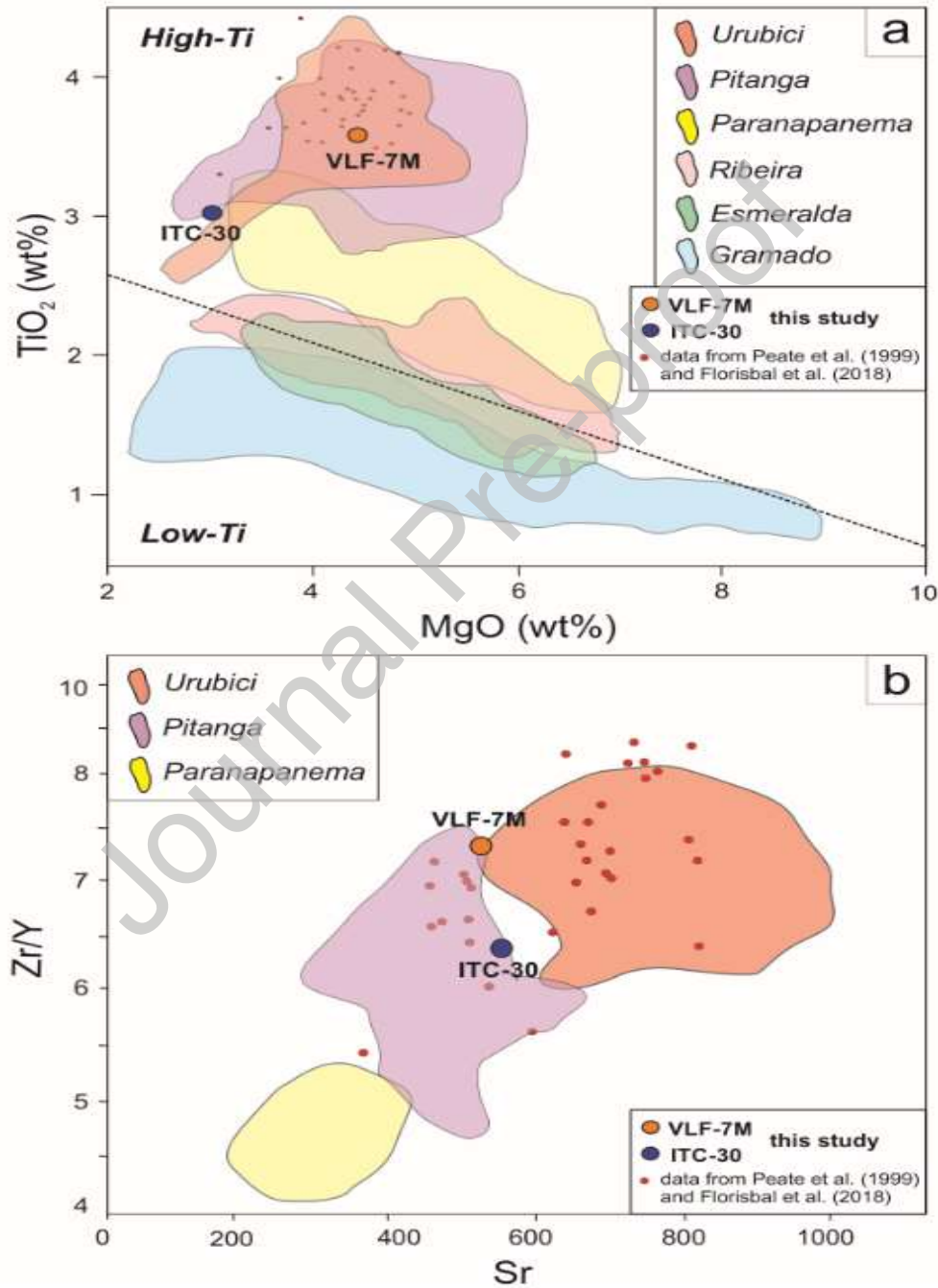


Figure 5: Concordia diagrams showing the results of U-Pb baddeleyite ID-TIMS geochronology of a-b) Florianópolis Dyke Swarm (VLF-07M) and Taió Sill (ITC-30) (2σ error ellipses). Reported ages are Th-corrected $^{206}\text{Pb}/^{238}\text{U}$ weighted mean ages.

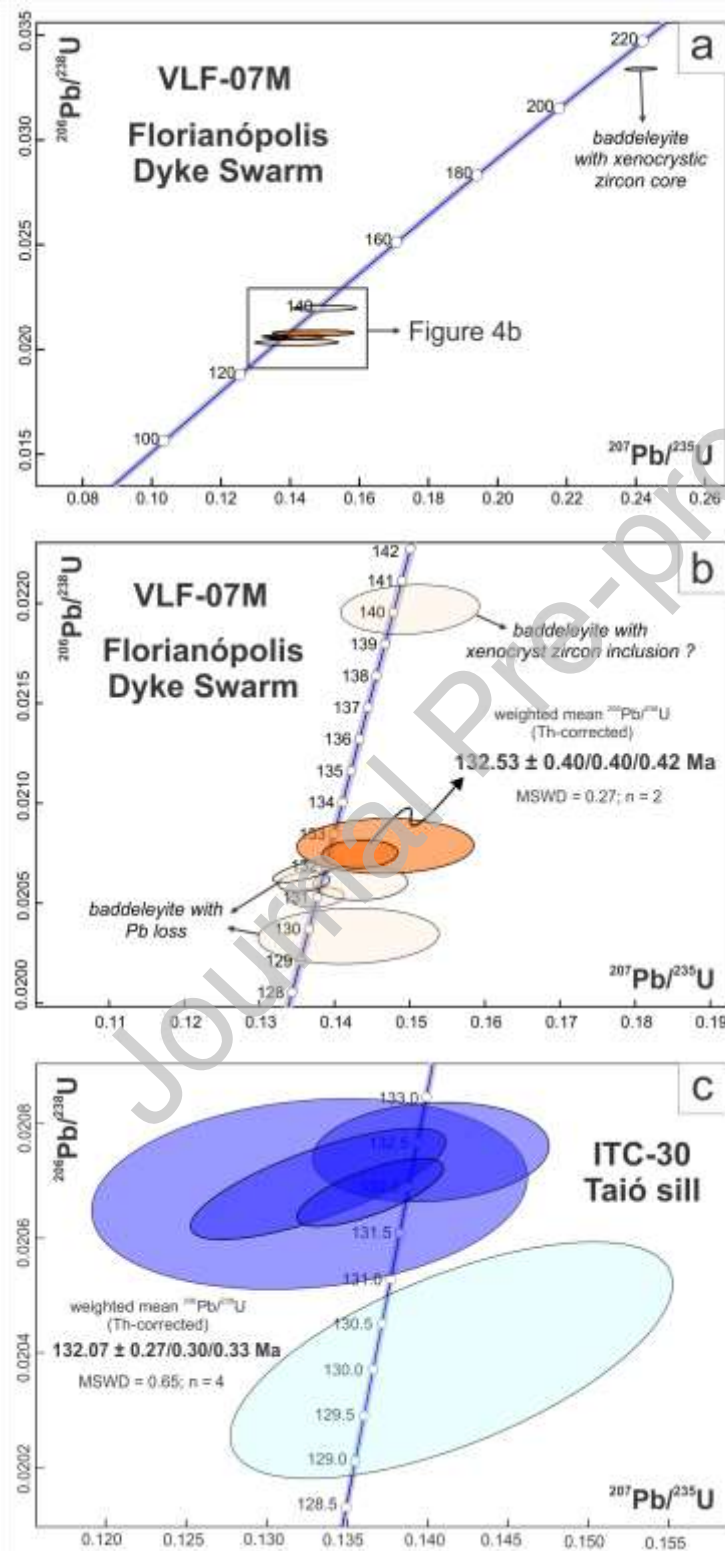


Figure 6: Rank-order plot of U-Pb baddeleyite ages from a high-Ti-Sr mafic intrusive rocks from the Paraná LIP in Brazil: a composite dyke (sample VLF-07M – Florianópolis Dyke Swarm) and a dolerite sill (sample ITC-30 – Taió Sill) emplaced in Permian-Triassic sedimentary rocks from the Paraná basin. Vertical bars represent single grain $^{206}\text{Pb}/^{238}\text{U}$ baddeleyite ages with 2σ uncertainties. Dark colored analyses are used to calculate a weighted average age (horizontal gray bar), that represent the emplacement ages of dyke and sill. Light colored analyses were discarded from weighted average age calculations due to suspected secondary Pb-loss (younger dates) and mixture of baddeleyite with a xenocrystic zircon component (older date).

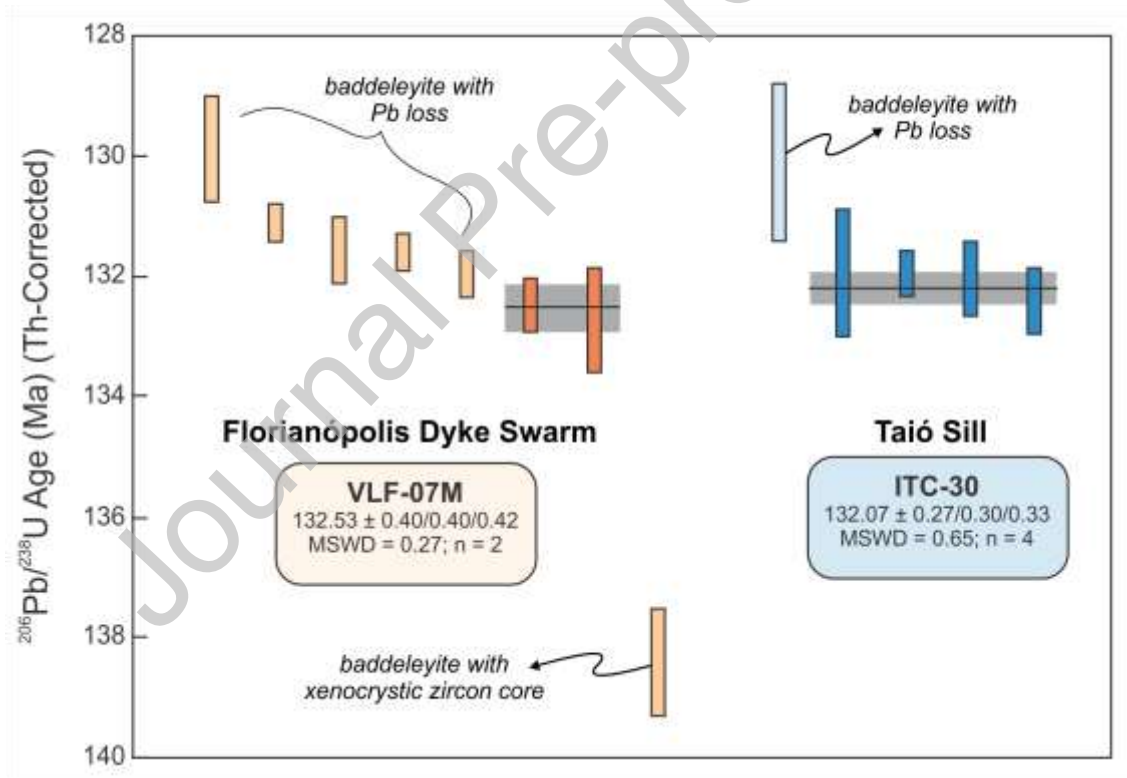


TABLE CAPTIONS

Table 1: New U-Pb ID-TIMS baddeleyite data from high-Ti-Sr mafic intrusive rocks from the Paraná LIP.

U-Pb baddeleyite geochronology data of high-Ti-Sr mafic intrusive rocks from the Paraná LIP

Sample	Composition				Isotopic Ratios						Dates (Ma)					Corr. Coeff.						
	U a	U (pg) g	Pb * (pg) b	Pb c (pg) g	P b * -	²⁰⁶ Pb e	²⁰⁶ Pb f	± 2 σ	²⁰⁷ Pb g	± 2 σ	²⁰⁷ Pb h	± 2 σ	²⁰⁶ Pb i	± 2 σ	²⁰⁷ Pb j		± 2 σ	²⁰⁶ Pb k	± 2 σ	²⁰⁷ Pb l	± 2 σ	
VLF-07M																						
VLF-07-B3	0.68	5.04	1.73	0.44	3.98	27.02	0.039	0.002	0.241	1.908	0.017	1.158	0.008	0.004	2.196	3.079	0.011	0.006	3.475	4.775	0.025	0.018
VLF-07-B5	0.87	3.08	0.77	0.69	1.13	94.96	0.021	0.006	0.142	8.647	0.005	8.858	0.008	0.005	1.809	1.508	0.008	0.007	3.490	7.807	0.013	0.009
VLF-07-B6	0.51	4.70	1.07	0.54	2.00	14.58	0.020	0.003	0.143	3.551	0.004	3.247	0.008	0.005	1.405	1.603	0.004	0.007	2.337	4.033	0.012	0.008
VLF-07-B7	0.15	4.50	0.80	0.52	1.55	11.73	0.020	0.002	0.145	4.509	0.002	4.528	0.005	0.008	1.155	1.611	0.005	0.009	3.556	5.511	0.008	0.005
VLF-07-B8	0.70	5.00	1.07	0.33	3.20	22.74	0.020	0.003	0.135	2.603	0.002	2.157	0.004	0.003	1.331	1.903	0.003	0.003	3.951	9.303	0.007	0.002
VLF-07-B9	0.85	5.08	1.11	0.48	2.32	16.70	0.020	0.006	0.136	3.669	0.002	3.900	0.008	0.000	1.399	1.385	0.003	0.009	3.995	9.775	0.009	0.004
VLF-07-B11	0.91	4.09	0.56	0.52	1.08	90.74	0.020	0.008	0.141	8.338	0.004	8.968	0.006	0.008	2.988	4.477	0.008	0.001	3.880	7.747	0.008	0.008
VLF-07-	0.60	5.67	1.07	0.36	3.21	21.20	0.020	0.002	0.137	2.648	0.002	2.535	0.003	0.003	1.303	1.303	0.003	0.003	3.103	6.303	0.001	0.001

B12	0	3			0	58	53	4	66	3	65	9	1.	3	0.	2	0.	1	1
	7	7			0	3	0	4	3	2	5	7	1	2	9	3	2	0	9
													1		6		0		
VLF-	0	5			1	91	0.0	0.	0.1	8.	0.0	8.	1	0	1	1	2	1	0
07-	.	4.	1.0	0.9	.	.4	20	6	46	0	51	0	3	.	9.	.	0.	4.	.
B15	0	7	6	7	0	29	78	6	74	2	22	2	2.	8	0	4	0	7	0
	9	6			9		6	1	9	0	7	6	3	7	4	2	3	1	3
ITC-																			
30																			
ITC-	0	2			2	18	0.0	0.	0.1	3.	0.0	3.	1	0	1	4	9	7	0
30-	.	1.	0.4	0.1	.	9.	20	2	36	3	47	1	3	.	2	4	4.	3.	.
B1	0	7	1	5	6	93	66	9	45	1	91	0	1.	3	9.	0	1	5	7
	2	7			6	1	3	0	7	6	8	8	9	8	8	4	8	9	4
													5						
ITC-	0	4			1	13	0.0	0.	0.1	5.	0.0	5.	1	0	1	7	3	1	0
30-	.	1.	0.2	0.1	.	9.	20	4	33	9	46	6	3	.	2	5.	4.	.	.
B10	0	8	2	2	9	06	67	7	24	6	75	0	2.	6	7.	1	8	4.	7
	8	3			1	7	7	6	5	4	8	4	0	2	0	2	0	1	7
													4					8	
ITC-	0	1			1	13	0.0	0.	0.1	5.	0.0	5.	1	0	1	6	1	1	0
30-	.	0.	0.8	0.4	.	9.	20	4	40	2	49	2	3	.	3.	5	0.	2.	.
B3	0	6	0	5	7	83	73	2	23	6	07	3	2.	5	2	7	3	7	0
	7	6			9	2	5	0	6	3	4	8	4	5	5	1	1	7	0
													0						
ITC-	0	8.	0.2	0.1	1	89	0.0	0.	0.1	1	0.0	1	1	1	1	2	2	4	0
30-	.	7	0	9	.	.3	20	8	32	0.	46	1	1.	.	6.	.	7.	2.	.
B8	0	4	0	0	0	82	66	1	68	5	59	2	9	0	5	1	4	8	1
	0				2	1	2	1	2	6	8	4	6	6	0	9	8	6	9
													8						
ITC-	0	1			0	79	0.0	1.	0.1	9.	0.0	9.	1	1	1	2	2	0	0
30-	.	1.	0.1	0.1	.	.6	20	0	41	7	50	1	0.	.	4.	.	1.	0.	.
B9	0	7	6	7	9	81	37	1	45	4	38	0	1	3	3	2	8	9	6
	5	6			8	0	9	7	0	7	3	0	0	1	4	6	5	4	6

^a Th contents calculated from radiogenic ²⁰⁸Pb and ²³⁰Th-corrected ²⁰⁶Pb/²³⁸U date of the sample, assuming concordance between U-Pb Th-Pb systems.

^b Total mass of radiogenic Pb.

^c Total mass of common Pb.

^d Ratio of radiogenic Pb (including ²⁰⁸Pb) to common Pb.

^e Measured ratio corrected for fractionation and spike contribution only.

^f Measured ratios corrected for fractionation, tracer, blank and, where applicable, initial common Pb.

^g Corrected for initial Th/U disequilibrium using radiogenic ²⁰⁸Pb and Th/U_[magma] = 3.50.

t_h Isotopic dates calculated using $\lambda_{238} = 1.55125E-10$ (Jaffey et al. 1971) and $\lambda_{235} = 9.8485E-10$ (Jaffey et al. 1971).

i % discordance = $100 - (100 * (^{206}\text{Pb}/^{238}\text{U date}) / (^{207}\text{Pb}/^{206}\text{Pb date}))$

Journal Pre-proof